

# A taxonomic reassessment of *Piramys auffenbergi*, a neglected turtle from the late Miocene of Piram Island, Gujarat, India

Gabriel S Ferreira<sup>Corresp., 1, 2</sup>, Saswati Bandyopadhyay<sup>3</sup>, Walter G Joyce<sup>Corresp. 4</sup>

<sup>1</sup> Faculdade de Filosofia, Ciências e Letras de Ribeirão Preto, Universidade de São Paulo, Ribeirão Preto, Brazil

<sup>2</sup> Fachbereich Geowissenschaften, Eberhard-Karls-Universität Tübingen, Germany

<sup>3</sup> Geological Studies Unit, Indian Statistical Institute, Kolkata, India

<sup>4</sup> Departement für Geowissenschaften, University of Friburg, Freiburg, Switzerland

Corresponding Authors: Gabriel S Ferreira, Walter G Joyce

Email address: gsferreira@usp.br, walter.joyce@unifr.ch

**Background.** *Piramys auffenbergi* was described as an emydine turtle based on a well-preserved skull retrieved from late Miocene deposits exposed on Piram Island, India. The description and figures provided in the original publication are vague and do not support assignment to Emydinae. This taxon has mostly been ignored by subsequent authors.

**Material & Methods.** We reexamine the holotype specimen and provide an extensive description and diagnosis for *Piramys auffenbergi* and included this taxon in a global character-taxon matrix for Pleurodira.

**Results.** The presence of a processus trochlearis pterygoidei conclusively shows pleurodiran affinities for *Piramys auffenbergi*. Inclusion of this taxon in a phylogenetic analysis retrieves it within Stereogenyini and as sister to the Asian taxa *Shweboemys pilgrimi* and *Brontochelys gaffneyi*.

**Discussion.** Our reexamination of the holotype of *Piramys auffenbergi* confidently rejects the original assessment of this taxon as an emydine testudinoid and conclusively shows affinities with the pleurodiran clade Stereogenyini instead. Even though most taxa from this lineage are thought to be coastal turtles, all Asian stereogenyines were collected from continental deposits, suggesting a more diverse paleoecology for the group.

1 A taxonomic reassessment of *Piramys auffenbergi*, a neglected turtle  
2 from the late Miocene of Piram Island, Gujarat, India

3

4 Gabriel S. Ferreira<sup>1,2</sup>, Saswati Bandyopadhyay<sup>3</sup>, Walter G. Joyce<sup>4</sup>

5

6 <sup>1</sup>Faculdade de Filosofia, Ciências e Letras de Ribeirão Preto, Universidade de São Paulo,

7 Ribeirão Preto, Brazil

8 <sup>2</sup>Fachbereich Geowissenschaften, Eberhard-Karls-Universität Tübingen, Tübingen, Germany

9 <sup>3</sup>Geological Studies Unit, Indian Statistical Institute, Kolkata, India

10 <sup>4</sup>Departement für Geowissenschaften, Universität Freiburg, Freiburg, Switzerland

11

12 \* Walter G. Joyce, walter.joyce@unifr.ch, walter.g.joyce@gmail.com

13

14 ABSTRACT

15 **Background.** *Piramys auffenbergi* was described as an emydine turtle based on a well-preserved  
16 skull retrieved from late Miocene deposits exposed on Piram Island, India. The description and  
17 figures provided in the original publication are vague and do not support assignment to  
18 Emydinae. This taxon has mostly been ignored by subsequent authors.

19 **Material & Methods.** We reexamine the holotype specimen and provide an extensive  
20 description and diagnosis for *Piramys auffenbergi* and included this taxon in a global character-  
21 taxon matrix for Pleurodira.

22 **Results.** The presence of a processus trochlearis pterygoidei conclusively shows pleurodiran  
23 affinities for *Piramys auffenbergi*. Inclusion of this taxon in a phylogenetic analysis retrieves it

24 within Stereogenyini and as sister to the Asian taxa *Shweboemys pilgrimi* and *Brontochelys*  
25 *gaffneyi*.

26 **Discussion.** Our reexamination of the holotype of *Piramys auffenbergi* confidently rejects the  
27 original assessment of this taxon as an emydine testudinoid and conclusively shows affinities  
28 with the pleurodiran clade Stereogenyini instead. Even though most taxa from this lineage are  
29 thought to be coastal turtles, all Asian stereogenyines were collected from continental deposits,  
30 suggesting a more diverse paleoecology for the group.

31

## 32 INTRODUCTION

33 *Piramys auffenbergi* was described by Prasad (1974) based on a single skull (GSI 18133)  
34 retrieved from Neogene sediments exposed on the small island of Piram, Gujarat State, India  
35 (Fig. 1). Prasad (1974) identified the taxon as an emydine, but the diagnosis and the description  
36 are general and do not reveal any emydine affinities. Today, only cryptodiran cheloniids,  
37 geoemydids (formerly part of Emydidae), testudinids, and trionychids occur in India (TTWG,  
38 2017), but stereogenyine pleurodires inhabited the area as recently as the Plio/Pleistocene  
39 (Gaffney et al., 2011).

40 Here we provide an extensive description and diagnosis of *Piramys auffenbergi* based on a  
41 reexamination of the holotype specimen. Phylogenetic analysis concludes that this taxon is a  
42 representative of Stereogenyini, a clade that includes other South Asian forms, namely the  
43 Plio/Pleistocene *Shweboemys pilgrimi* Swinton, 1939 from Myanmar, and the late Oligocene  
44 *Brontochelys gaffneyi* (Wood, 1970) from Pakistan. We also provide an updated account of the  
45 paleoecology and biogeography of the group, concluding that, although they were most likely

46 adapted (or at least highly tolerant) to salty waters, stereogenyines were still restricted  
47 geographically and not as widespread as modern sea turtles.

48 Institutional abbreviations.— GSI, Geological Survey of India, Kolkata, India.

49

## 50 SYSTEMATIC PALEONTOLOGY

51 PLEURODIRA Cope, 1865

52 PELOMEDUSOIDES Broin, 1988

53 PODOCNEMIDIDAE Cope, 1868

54 STEREOGENYINI Gaffney et al., 2011

55 STEREOGENYITA Gaffney et al., 2011

56 *Piramys auffenbergi* Prasad, 1974

57 Holotype.— GSI 18133, a partial skull (Prasad, 1974, figs. 2–4, pl. 3.1; Figure 2).

58 Type locality and horizon.— Piram Island (Fig. 1), Gulf of Khambhat (formerly Gulf of  
59 Cambay), Gujarat, India; conglomerate beds, middle Siwaliks (Prasad, 1974), Dhok Pathan age,  
60 late Miocene (Nanda, Sehgal & Chauhan, 2017).

61 Referred material.— No specimens have been referred to date.

62 Diagnosis.—*Piramys auffenbergi* can be diagnosed as a representative of Pleurodira by the  
63 presence of the processus trochlearis pterygoidei and of Pelomedusoides by the absence of nasal  
64 bones. *Piramys auffenbergi* can be further diagnosed as a representative of Stereogenyini by the  
65 small entrance to the antrum postoticum, the condylus mandibularis projecting ventrally from the  
66 cavum tympani, and the posteriorly broad skull, and as a member of Stereogenyita closer to  
67 *Shweboemys pilgrimi* and *Stereogenys cromeri* by a median notch in the upper jaw. *Piramys*  
68 *auffenbergi* is distinguished from the other members of Stereogenyini by the following

69 combination of characters: a pinched snout (not present in *Latentemys plowdeni* Gaffney et al.,  
70 2011, *Bairdemys venezuelensis* [Wood & Díaz de Gamero, 1971], and *B. sanchezi* Gaffney et al.,  
71 2008), a deep interorbital groove on the prefrontal and frontal (otherwise present in *Cordichelys*  
72 *antiqua* [Andrews, 1903]), foramen nervi trigemini located above the level of the sulcus  
73 palatinopterygoideus (in contrast to the more ventrally displaced foramen nervi trigemini in  
74 *Shweboemys pilgrimi* and *Brontochelys gaffneyi*), the lower temporal emargination rising above  
75 the ventral level of the orbit (shallower in *C. antiqua* and unknown for other Stereogenyita), and  
76 the foramen stapedio-temporale placed anteriorly (autapomorphic character).

77

#### 78 DESCRIPTION

79 Preservation.—The skull was likely buried intact but suffered much weathering damage more  
80 recently. The bone is nevertheless of good quality and sutures are well preserved. The palate and  
81 ventral aspects of the basicranium are still obscured by matrix, but the dermatocranium and the  
82 dorsal parts of the basicranium are exposed (Fig. 2). The margins of the external nares and the  
83 median portions of the labial margins are damaged, but the remaining margins likely  
84 approximate their original outlines. The temporal roofing, by contrast, is massively eroded and  
85 the extent of the upper temporal emarginations can therefore not be assessed anymore. Much of  
86 the postorbitals, parietals, quadratojugals, squamosals, and the supraoccipital are missing. Faint  
87 scute sulci are apparent on the postorbitals and parietals (Fig. 2A).

88 Prefrontal.—The prefrontals are relatively small, paired elements that form the anterodorsal  
89 aspects of the orbit and the anterior third of the narrow interorbital space. The anterior margins  
90 are damaged, but the prefrontals likely formed the dorsal roof of the external nares, as nasals  
91 were absent. The prefrontals contact the frontals posteriorly along a straight, transverse suture,

92 the maxillae ventrally along a straight, horizontal suture, and one another along a straight,  
93 median suture. The descending branch of the prefrontal contacts the frontal posteriorly and the  
94 maxilla ventrally, but potential, more-distal contacts with the vomer and palatine are obscured by  
95 matrix (Fig. 2C). The prefrontals jointly form a deep, median groove on the dorsal skull surface  
96 (Fig. 2A).

97 Frontal.—The frontals are the only bones that are undamaged. The dorsal plate of the frontals  
98 forms the posterior two thirds of the interorbital space and posterodorsal margins of the  
99 anterolaterally facing orbits. The frontals contact the prefrontals anteriorly along a straight,  
100 transverse suture, the postorbitals laterally along parasagittal sutures of uneven length, the  
101 parietals posteriorly along straight, transverse sutures, and one another along a straight, median  
102 suture. Within the orbits, the frontals contact the prefrontals anteriorly and the postorbitals  
103 laterally. The median groove formed by the prefrontals continues posteriorly onto the frontals  
104 (Fig. 2A), but fades to oblivion towards the posterior margins of these elements.

105 Parietal.—Symmetric damage to the dorsal plate of the parietal creates the illusion that the  
106 parietals are relatively small elements that define the margins of well-developed upper temporal  
107 emarginations, but all margins show signs of damage and the extent of this emargination cannot  
108 be assessed with any confidence. It is therefore only clear that the dorsal plates of the parietals  
109 contact the frontals anteriorly along straight, transverse sutures and the postorbitals along  
110 oblique, anterolateral sutures. Together with the postorbitals, the parietals form a pair of sulci  
111 that converge towards the posterior and that likely trace the outline of a large internarial scute  
112 (scute ii of Ferreira et al., 2015) that covered the prefrontals, frontals, and the medial portions of  
113 the postorbitals and parietals. The descending process of the parietals contacts the pterygoid  
114 anterior to the foramen nervi trigemini, forms the dorsal margin of this foramen, and contacts the

115 prootic and supraoccipital posterior to it (Fig. 2A). The foramen nervi trigemini is located above  
116 the level of the sulcus palatinopterygoideus and is well separated from the foramen stapedio-  
117 temporale by the prootic (Fig. 2C). More anterior contacts, if present, are obscured by matrix.

118 Postorbital.—The posterior margins of the postorbitals show signs of damage and it is  
119 therefore not possible to assess if they originally contributed to the upper temporal  
120 emarginations, although the thickness of their damaged margins makes this implausible.  
121 However, as the intact posterior margins converge, it is unlikely that they were significantly  
122 larger than preserved. The dorsal plates of the postorbitals at least contact the frontals medially,  
123 the parietals posteromedially, the jugals ventrally, and the quadratojugals posterolaterally. The  
124 descending process of the postorbital forms much of the posterior wall of the orbit, but its distal  
125 contacts are obscured by matrix. We are not able to discern a dorsal pocket within the upper  
126 limits of the posterior wall of the orbit.

127 Jugal.—The jugals are relatively large elements that form the posteroventral aspects of the  
128 orbit. Although the posteroventral aspects are damaged on both sides, enough is preserved to  
129 indicate that a well-developed lower temporal emargination is developed that rises to the level of  
130 the lower third of the orbit and that is anterodorsally framed by the jugals (Fig. 2B). The jugals  
131 contact the postorbitals dorsally along horizontal sutures, the quadratojugal posteriorly along a  
132 transverse suture, and the maxillae anteroventrally along a slightly oblique suture. The jugals  
133 contact the maxilla anteriorly and the postorbitals laterally on the surface of the skull, but matrix  
134 obscures possible contacts within the orbit.

135 Quadratojugal.—Only a fragment of the quadratojugal remains on the right side of the skull  
136 (Fig. 2B). It is therefore unclear if the quadratojugal contributes to the upper or lower temporal  
137 emarginations, although a contribution to the lower temporal emargination appears highly likely.

138 Only a short, anteromedial contact is preserved with the postorbital, an elongate anterior contact  
139 with the jugal, and remnants of the posterior contact of the quadrate anterior to the cavum  
140 tympani.

141 Squamosal.—A fragment of the right squamosal is available at the back of the skull (Fig. 2A).  
142 This fragment contacts the quadrate anterolaterally and the opisthotic anteromedially within the  
143 upper temporal fossa. A likely contribution of the squamosal to the region posterior to the cavum  
144 tympani cannot be discerned from that of the quadrate. However, the massive nature of the  
145 damaged quadrates suggests that the squamosal did not contribute to the antrum postoticum.

146 Premaxilla.—The anterior tip of the skull is damaged, but the median, cleft like notch appears  
147 to be genuine, as much of the left labial margin is intact (Fig. 2D). We are unable to discern the  
148 contacts, or even the presence, of premaxillae.

149 Maxilla.—The maxillae can only be observed in anterior and lateral views, as the palate is  
150 hidden by matrix. On the skull surface, the high maxillae contact the jugals below the orbit along  
151 transverse sutures and the prefrontals dorsally along horizontal suture. These contacts can  
152 partially be traced within the orbits, but matrix obscures their full extent. It is unclear if an  
153 anterior contact is developed with the premaxillae. Likely contacts with the palatines are  
154 obscured by matrix. The maxillae otherwise form the labial margins of the jaw, the anteroventral  
155 margins of the orbit, and the lateral margin of the broad external nares.

156 Pterygoid.—Only the most lateral and medial tips of the left pterygoid are visible (Fig. 2A).  
157 Medially, the pterygoid forms the anterior margin of the foramen nervi trigemini and contacts the  
158 parietal dorsally. Laterally, the pterygoid forms the processus trochlearis pterygoidei, of which  
159 only the damaged lateral tip is free from matrix (Fig. 2C). The process is perpendicular to the  
160 midline and almost vertical in lateral view.

161 Prootic.—Only the left prootic can be observed in dorsal view and its sutures are obscured by  
162 localized damage to the surface of the skull. The left prootic clearly contacts the descending  
163 process of the parietal anteromedially and the quadrate laterally. Contacts are certainly present  
164 with the supraoccipital posteromedially and the opisthotic posteriorly, but their orientation and  
165 size cannot be estimated with confidence. The left prootic partially roofs the foramen nervi  
166 trigemini and together with the left quadrate forms the foramen stapedio-temporale, which is  
167 situated at the anterior margin of the otic capsule and oriented anteriorly (Fig. 2A).

168 Opisthotic.—Only the external aspects of the opisthotics can be observed. Within the upper  
169 temporal fossa, the opisthotics contact the supraoccipital anteromedially, the quadrate  
170 anterolaterally, the squamosal posterolaterally, and the exoccipital posteromedially.

171 Quadrate.—Much of the quadrates remain on both sides of the skull, but most surfaces are  
172 damaged, making it difficult to discern its original shapes and contacts. At the very least, the  
173 quadrate contacts the quadratojugal anterodorsally and the squamosal posteriorly along the skull  
174 surface. Within the upper temporal fossa, the quadrate contacts the squamosal posteriorly, the  
175 opisthotic posteromedially, and the prootic anteromedially. Although damage to the middle ear is  
176 significant, it is apparent that the quadrates fully enclosed the incisura columella auris and  
177 Eustachian tube and that the quadrates fully formed the highly reduced antrum postoticum.  
178 However, matrix obscures the presence of a possible precolumellar fossa. In lateral view (Fig.  
179 2C), the mandibular condyle of the quadrate projects ventrally, beyond the ventral outline of the  
180 cavum tympani.

181 Supraoccipital.—The supraoccipital is heavily eroded and some of its contacts are obscured  
182 by damage. It is therefore not possible to assess its possible contribution to the dorsal skull roof  
183 or the length of the supraoccipital crest. Within the upper temporal fossa, the supraoccipital

184 certainly contacts the parietal anteromedially, the prootic anterolaterally, the opisthotic  
185 posterolaterally, and the exoccipital posteriorly. In posterior view, the supraoccipital roofs the  
186 foramen magnum and contacts the exoccipitals ventrally.

187 Exoccipital.—The exoccipitals are both present, but their ventral portions are obscured by  
188 matrix. These bones form the lateral margins of the foramen magnum, contact the supraoccipital  
189 dorsally, the opisthotic anterolaterally, but their likely ventral contacts with the basioccipital are  
190 obscured. Although the occipital condyle is heavily damaged, the sulcus left by the contact  
191 between the exoccipitals laterally and the basioccipital ventrally are still visible (Fig. 2E).

192

## 193 MATERIAL & METHODS

194 We integrated the holotype of *Piramys auffenbergi* into the phylogenetic matrix of Ferreira et al.  
195 (2018) to assess its relationships to other pleurodires. Obtaining CT scans of this specimen  
196 would have been desirable, as this would help clarify the morphology of the palate, but was not  
197 feasible within the context of this study due to logistic hurdles. The matrix was modified through  
198 the addition of a new character (ch. 245: PM, median notch on upper jaw; see Supplementary  
199 Files) and by updating the scorings of some taxa based on new observations by one the authors  
200 (GSF) (see Supplementary Files for full list of changes). As in the original analysis (Ferreira et  
201 al., 2018), twelve characters (14, 18, 19, 71, 95, 96, 99, 101, 119, 129, 174, 175) were interpreted  
202 as forming morphoclines and were ordered in the analysis. The resulting matrix was analyzed in  
203 TNT v. 1.5 (Goloboff & Catalano, 2016) using a traditional search with 2000 replicates of  
204 Wagner trees, random seed set to 0, branch-swapping algorithm Tree Bisection Reconnection  
205 (TBR), hold = 0, and collapsing zero-length branches according to rule '1'. The most  
206 parsimonious trees (MPTs) were subject to a second round of TBR and a strict consensus was

207 obtained from the resulting MPTs. Consistency (CI) and Retention (RI) indexes, Bremer support,  
208 and resampling values (bootstrap and jackknife, using 1000 resamples for calculating absolute  
209 and difference of frequencies; Goloboff et al., 2003) were retrieved using implemented functions  
210 in TNT.

211

## 212 RESULTS

213 The search yielded 270 MPTs with 1134 steps (CI=0.288; RI=0.748). The strict consensus (see  
214 Supplementary Files) differs slightly from the results of Ferreira et al. (2018) by yielding a  
215 polytomy in the clade that includes the extant *Erymnochelys madagascariensis* (Grandidier  
216 1867) and *Peltocephalus dumerilianus* (Schweigger 1812). *Piramys auffenbergi* is retrieved with  
217 relatively high support (Bremer support = 2; see Supplementary Files) inside Stereogenyini, in a  
218 polytomy with *Stereogenys cromeri* Andrews, 1901 and *Shweboemys pilgrimi* (Fig. 3).

219

## 220 DISCUSSION

### 221 **Alpha taxonomy and phylogenetic relationships**

222 Prasad (1974) documented in the original description and figures of the holotype of *Piramys*  
223 *auffenbergi* the presence of large nasals, elongate prefrontals, small frontals that do not  
224 contribute to the orbits, and deep upper temporal emarginations. Prasad (1974) unfortunately did  
225 not explain why he felt *Piramys auffenbergi* to be an emydine, but we note that the presence of  
226 nasals is neither consistent with an assignment to Emydinae in particular, nor Testudinoidea  
227 more generally, as testudinoids universally lack nasal bones (Gaffney, 1979). Our re-examination  
228 of the type specimen allows us to better evaluate the cranial morphology and taxonomic affinities  
229 of this taxon and to present a more detailed list of diagnostic characters.

230 The most apparent differences in our interpretation of the skull is that nasals are absent, that  
231 the prefrontals are situated at the front of the orbits, that the frontals broadly contribute to the  
232 orbits, that the margin of the upper temporal emargination is not preserved, and that a trochlear  
233 process is present on the pterygoid. The presence of a trochlear process of the pterygoid  
234 combined with the absence of nasals clearly hint at pelomedusoid affinities for *Piramys*  
235 *auffenbergi* (Gaffney, 1979; Gaffney, Tong & Meylan, 2006; Joyce, 2007). The trochlear process  
236 is almost completely embedded in matrix, but its lateral tip can be seen anterior to the otic  
237 capsule (Fig. 2C).

238 The posteriorly broadened skull, small anterior opening of the antrum postoticum, and a  
239 mandibular condyle projecting ventrally from the cavum tympani in lateral view (Fig. 2C)  
240 suggest stereogenyine affinities (Gaffney et al., 2011; Ferreira et al., 2015). The results of our  
241 phylogenetic analysis (Fig. 3) support this initial hypothesis, even though *Piramys auffenbergi* is  
242 scored as “unknown” for several characters that support the monophyly of Stereogenyini. The  
243 majority of characters that resolve relationships within Stereogenyini, e.g., presence of a  
244 secondary palate with a midline cleft (Gaffney et al., 2011; Ferreira et al., 2015), refer to features  
245 in the ventral region of the skull. Unfortunately, this region is covered by matrix in GSI 18133,  
246 hampering a more detailed account of its taxonomic affinities. Nevertheless, the pinched snout  
247 (ch. 41, state 1), premaxillae protruding anteriorly beyond the dorsal edge of the apertura narium  
248 externa (ch. 43, state 1), the small opening of the antrum postoticum (ch. 86, state 2), the ventral  
249 projection of the mandibular condyle (ch. 90, state 1), and the median notch in the upper jaw (ch.  
250 246, state 2) supports *Piramys auffenbergi* as a Stereogenyini with close affinities to *Stereogenys*  
251 *cromeri* and *Shweboemys pilgrimi* (Fig. 3).

252 Comparisons of *Piramys auffenbergi* with other Asian stereogenyines reveal osteological and  
253 chronological distinctness. The Bugti Hills in Pakistan, the type locality of *Brontochelys*  
254 *gaffneyi*, are now considered to be late Oligocene in age (Welcome et al., 2001; see discussion in  
255 the next section) whereas the Irrawaddy Beds in Myanmar, the type locality of *Shweboemys*  
256 *pilgrimi*, are thought to be Pliocene/Pleistocene age (Thein, Nu & Pyone, 2012). The sediments  
257 exposed on Piram Island are dated as late Miocene (Nanda, Sehgal & Chauhan, 2017) and  
258 *Piramys auffenbergi* therefore is temporally distinct. *Piramys auffenbergi* differs from  
259 *Brontochelys gaffneyi* by the presence of a pinched snout, anterodorsally facing orbits, and a  
260 median notch in the upper jaw. On the other hand, *Piramys auffenbergi* differs from *Shweboemys*  
261 *pilgrimi* by the presence of an interorbital space that is narrower than the diameter of the orbits  
262 and the straight prefrontal-frontal suture. Furthermore, *Piramys auffenbergi* can be distinguished  
263 from both other Asian stereogenyines by the presence of a narrow interorbital groove, the more  
264 posterodorsally located foramen nervi trigemini, and the anterior, instead of dorsal, opening of  
265 the foramen stapedio-temporale. We are therefore able to confirm the validity of *Piramys*  
266 *auffenbergi*, though not as a testudinoid cryptodire, but rather as a podocnemidid pleurodire.

267

### 268 **Paleoecology and biogeography**

269 Members of Stereogenyini are currently thought to be durophagous, because they have broad and  
270 flat triturating surfaces combined with a secondary palate (Ferreira et al., 2015), features that are  
271 prevalent among extant turtles with durophagous dietary preferences (Foth, Rabi & Joyce, 2017).  
272 The palate is not exposed in the holotype of *Piramys auffenbergi* and we are therefore not able to  
273 assess the diet of this taxon with confidence. However, the high maxillae, anterodorsally oriented  
274 orbits, and posteriorly broadened skull with space for well-developed adductor muscles (Fig. 3)

275 are features consistent with this life style. Considering the placement of *Piramys auffenbergi*  
276 within Stereogenyini we therefore predict the presence of durophagous features in this taxon as  
277 well.

278 Members of Stereogenyini are furthermore thought to have had a marine, or at least coastal,  
279 lifestyle based on limb morphology (Weems & Knight, 2013), shell morphology (Pérez-García,  
280 2017), and depositional environments (Ferreira et al., 2015). Although most stereogenyine taxa  
281 have indeed been recovered from sediments that represent coastal or open sea depositional  
282 environments (Ferreira et al., 2015), we here note that all known Asian stereogenyines were  
283 collected from continental deposits, at least as indicated by the prevalence of terrestrial mammals  
284 in combination with fresh water aquatic fish and reptiles. In particular, the type of *Brontochelys*  
285 *gaffneyi* was collected from late Oligocene (not Miocene as reported Wood, 1970; Gaffney et al.,  
286 2011) continental sediments exposed in the region of Dera Bugti, Pakistan (Marivaux et al.,  
287 1999; Welcome et al., 2001), *Shweboemys pilgrimi* from the continental Plio/Pleistocene  
288 Irrawaddy Beds of Myanmar (Thein, Nu & Pyone, 2012), and, as demonstrated herein, *Piramys*  
289 *auffenbergi* from the continental late Miocene middle Siwaliks of India (Nanda, Sehgal &  
290 Chauhan, 2017). However, the more marine adapted African representatives of the Tethyan clade  
291 Stereogenyita, in particular *Stereogenys cromeri* and *Lemurchelys diasphax*, indicate a certain  
292 amount of ecological fluidity within the group. Bothremydids, another clade of pelomedusoid  
293 pleurodires, also present a combination of marine and continental forms (e.g., Rabi, Tong &  
294 Botfalvai, 2012), suggesting that a high tolerance to saline waters may be a more widespread  
295 feature among side-necked turtles. This is also hinted at by experimental analyses (Bower et al.,  
296 2016). However, as deltaic and marine sediments often interfinger finely and as estuarine and  
297 coastal turtles are expected to be found in numerous coastal facies, we suggest that the available

298 data is not sufficient to establish a rigorous pattern for the moment. Nevertheless, the fact that  
299 our phylogenetic analysis retrieves two geographically separated clades, the Tethyan  
300 Stereogenyita and the South American Bairdemydita, suggests that the even more salt tolerant  
301 forms were not highly marine, as greater amounts of dispersal and less endemism were otherwise  
302 to be expected.

303 Despite the broad geographic distribution of stereogenyines across North and South America,  
304 Africa, and India, they did not achieve the degree of cosmopolitanism seen in modern sea turtles  
305 (Chelonioidea; TTWG 2017). Instead, it appears that they were restricted to equatorial and  
306 subtropical regions of the northern hemisphere (Fig. 4). This hints at the possibility that their  
307 distribution was limited by cooler temperatures outside of the tropics.

308

#### 309 CONCLUSIONS

310 Our re-examination of the type specimen revealed the presence of pelomedusoid features in  
311 *Piramys auffenbergi*, e.g., presence of a pterygoid trochlear process in combination with the  
312 absence of nasals. Another set of characters suggested a Stereogenyini affinity which was  
313 confirmed by the results of our phylogenetic analysis of a global matrix for Pleurodira. *Piramys*  
314 *auffenbergi* is nested closer to the other Asian stereogenyines *Brontochelys gaffneyi* and  
315 *Shweboemys pilgrimi*. The phylogenetic position and provenance of *Piramys auffenbergi* is in  
316 accordance with the Stereogenyini broad geographic distribution and proposed high dispersal  
317 capability, but the relations within this lineage, with a South American and an African/Asian  
318 clade, suggest they were not as cosmopolitan as modern sea turtles.

319

#### 320 ACKNOWLEDGEMENTS

321 We would like to thank all officials and supporting staff at the Curatorial Division of the  
322 Geological Survey of India and of the Indian Museum for generously providing access to  
323 collections under their care, in particular Senior Geologist A. Bhattacharya, Senior Geologist M.  
324 R. Moulick, and Senior Geologist A. K. Mondal. The editor, Virginia Abdala, and the reviewers,  
325 Juliana Sterli, Márton Rabi and Torsten Scheyer, are thanked for insightful comments that helped  
326 improve the quality of the manuscript.

327

## 328 REFERENCES

- 329 **Andrews CW. 1901.** Preliminary note on some recently discovered extinct vertebrates from  
330 Egypt (Part II). *Geological Magazine* **8**:436–444.
- 331 **Andrews CW. 1903.** On some pleurodiran chelonians from the Eocene of the Fayum, Egypt.  
332 *Annals and Magazine of Natural History Series* **7**:115–122.
- 333 **Bower DS, Scheltinga DM, Clulow S, Clulow J, Franklin CE, Georges A. 2016.** Salinity  
334 tolerances of two Australian freshwater turtles, *Chelodina expansa* and *Emydura macquarii*  
335 (Testudinata: Chelidae). *Conservation Physiology* **4**:cow042.
- 336 **Broin F. 1988.** Les tortues et le Gondwana. Examen des rapports entre le fractionnement du  
337 Gondwana et la dispersion géographique des tortues pleurodires à partir du Crétacé. *Studia*  
338 *Palaeocheloniologica* **2**:103–142.
- 339 **Cope ED. 1865.** Third contribution to the herpetology of tropical America. *Proceedings of the*  
340 *Academy of Natural Sciences of Philadelphia* **1865**:185–198.
- 341 **Cope ED. 1868.** On the origin of genera. *Proceedings of the Academy of Natural Sciences of*  
342 *Philadelphia* **1868**:242–300.

- 343 **Dacqué E. 1912.** Die fossilen Schildkröten Aegyptens. *Geologische und Palaeontologische*  
344 *Abhandlungen* **14**:275–337.
- 345 **Ferreira GS, Bronzati M, Langer MC, Sterli J. 2018.** Phylogeny, biogeography and  
346 diversification patterns of side-necked turtles (Testudines: Pleurodira). *Royal Society Open*  
347 *Science* **5**:171773 DOI 10.1098/rsos.171773.
- 348 **Ferreira GS, Rincón AD, Solórzano A, Langer MC. 2015.** The last marine pelomedusoids  
349 (*Testudines: Pleurodira*): a new species of *Bairdemys* and the paleoecology of *Stereogenyina*.  
350 *PeerJ* **3**:e1063 DOI 10.7717/peerj.1063.
- 351 **Foth C, Rabi M, Joyce WG. 2017.** Skull shape variation in recent and fossil Testudinata and its  
352 relation to habitat and feeding ecology. *Acta Zoologica* **98**:310–325 DOI 10.1111/azo.12181.
- 353 **Gaffney ES. 1979.** Comparative cranial morphology of recent and fossil turtles. *Bulletin of the*  
354 *American Museum of Natural History* **164**:65–376.
- 355 **Gaffney ES, Meylan PA, Wood RC, Simons E, Campos DA. 2011.** Evolution of the side-  
356 necked turtles: the Family Podocnemididae. *Bulletin of the American Museum of Natural*  
357 *History* **350**:1–237 DOI 10.1206/350.1.
- 358 **Gaffney ES, Scheyer TM, Johnson KG, Bocquentin J, Aguilera OA. 2008.** Two new species  
359 of the side necked turtle genus, *Bairdemys* (Pleurodira, Podocnemididae), from the Miocene  
360 of Venezuela. *Paläontologische Zeitschrift* **82**:209–229 DOI 10.1007/BF02988411.
- 361 **Gaffney ES, Tong H, Meylan PA. 2006.** Evolution of the side-necked turtles: the families  
362 Bothremydidae, Euraxemydidae, and Araripemydidae. *Bulletin of the American Museum of*  
363 *Natural History* **300**:1–700 DOI 10.1206/0003-0090(2006)300[1:EOTSTT]2.0.CO;2.

- 364 **Gaffney ES, Wood RC. 2002.** *Bairdemys*, a new side-necked turtle (Pelomedusoides:  
365 Podocnemididae) from the Miocene of the Caribbean. *American Museum Novitates* **3359**:1–  
366 28 DOI 10.1206/0003-0082(2002)359<0001:BANSNT>2.0.CO;2.
- 367 **Goloboff PA, Catalano SA. 2016.** TNT version 1.5, including a full implementation of  
368 phylogenetic morphometrics. *Cladistics* **32**:221–238 DOI 10.1111/cla.12160.
- 369 **Goloboff PA, Farris JS, Källersjö M, Oxelman B, Ramírez MJ, Szumik CA. 2003.**  
370 Improvements to resampling measures of group support. *Cladistics* **19**:324–332 DOI  
371 10.1111/j.1096-0031.2003.tb00376.x
- 372 **Grandidier A. 1867.** Liste des reptiles nouveaux découverts, en 1866, sur la côte sud-ouest de  
373 Madagascar. *Revue et Magasin de Zoologie Pure et Appliquée* **19**:232–234.
- 374 **Joyce WG. 2007.** Phylogenetic relationships of Mesozoic turtles. *Bulletin of the Peabody*  
375 *Museum of Natural History* **48**:3–102.
- 376 **Marivaux L, Vianey-Liaud M, Welcomme J-L. 1999.** Première découverte de Cricetidae  
377 (Rodentia, Mammalia) Oligocènes dans le synclinal Sud de Gandoï (Bugti Hills,  
378 Balouchistan, Pakistan). *Comptes Rendus de l'Académie des Sciences* **329**:839–844.
- 379 **Nanda AC, Sehgal RK, Chauhan PR. 2017.** Siwalik-age faunas from the Himalayan Foreland  
380 Basin of South Asia. *Journal of Asian Earth Sciences* **162**:54–68 DOI  
381 10.1016/j.jseas.2017.10.035.
- 382 **Pérez-García A. 2017.** New information and establishment of a new genus for the Egyptian  
383 Paleogene turtle '*Stereogenys*' *libyca* (Podocnemididae, Erymnochelyinae). *Historical*  
384 *Biology* 1–11 DOI 10.1080/08912963.2017.1374383.
- 385 **Prasad KN. 1974.** The vertebrate fauna from Piram Island, Gujarat, India. *Memoires of the*  
386 *Geological Survey of India, New Series* **41**:1–23.

- 387 **Rabi M, Tong H, Botfalvai G. 2012.** A new species of the side-necked turtle *Foxemys*  
388 (Pelomedusoides: Bothremydidae) from the Late Cretaceous of Hungary and the historical  
389 biogeography of the Bothremydini. *Geological Magazine* **149**:662–674.
- 390 **Schweigger AF. 1812.** Prodrromus Monographiae Cheloniorum. *Konigsberger Archiv für*  
391 *Naturwissenschaft und Mathematik* **1**:406–458.
- 392 **Swinton WE. 1939.** A new fresh-water tortoise from Burma. *Records of the Geological Survey*  
393 *of India* **74**:548–551.
- 394 **Thein ZMM, Nu TT, Pyone WW. 2012.** Lithofacies and depositional environment of the  
395 Irrawaddy Formation in Myogintha Area, Pauk Township, Magway region. *Universities*  
396 *Research Journal* **5**:69–82.
- 397 **TTWG [Turtle Taxonomy Working Group]. 2017.** Turtles of the world: annotated checklist  
398 and atlas of taxonomy, synonymy, distribution, and conservation status (8th ed). *Chelonian*  
399 *Research Monographs* **7**:1–292.
- 400 **Weems RE, Knight JL. 2013.** A new species of *Bairdemys* (Pelomedusoides: Podocnemididae)  
401 from the Oligocene (Early Chattian) Chandler Bridge Formation of South Carolina, USA, and  
402 its paleobiogeographic implications for the genus. In: Brinkman D, Holroyd P, Gardner J, eds.  
403 *Morphology and evolution of turtles, Vertebrate paleobiology and paleoanthropology series.*  
404 Netherlands: Dordrecht, 289–303.
- 405 **Welcome J-L, Benammi M, Crochet J-Y, Marivaux L, Métais G, Antoine P-O, Baloch I.**  
406 **2001.** Himalayan forelands: paleontological evidence for Oligocene detrital deposits in the  
407 Bugti Hills (Balochistan, Pakistan). *Geological Magazine* **138**:397–405.
- 408 **Wood RC. 1970.** A review of the fossil Pelomedusidae (Testudines, Pleurodira) of Asia.  
409 *Breviora* **357**:1–24.

410 **Wood RC, Díaz de Gamero ML. 1971.** *Podocnemis venezuelensis*, a new fossil pelomedusid  
411 (Testudines, Pleurodira) from the Pliocene of Venezuela and a review of the history of  
412 *Podocnemis* in South America. *Breviora* **376**:1–23.

413

414 **Figure 1: The type locality of *Piramys auffenbergi*.**

415 (A) A simplified map of India. Gujarat State is highlighted in purple, all other states in various  
416 shades of grey. (B) Detailed view of the Gulf of Khambhat. Piram Island is highlighted in purple.

417

418 **Figure 2: GSI 18133, *Piramys auffenbergi*, holotype, late Miocene of Piram Island, Gujarat,**  
419 **India.**

420 Photographs and illustrations of specimen in (A) dorsal, (B) right lateral, (C) left lateral, (D)  
421 anterior, and (E) posterior views. Abbreviations: *cm*, condylus mandibularis; *et*, Eustachian tube;  
422 *fmt*, foramen nervi trigemini; *fr*, frontal; *fst*, foramen stapedio-temporale; *ju*, jugal; *mx*, maxilla;  
423 *oc*, occipital condyle; *op*, opisthotic; *pa*, parietal; *pf*, prefrontal; *po*, postorbital; *pr*, prootic; *ptp*,  
424 processus trochlearis pterygoidei; *qj*, quadratojugal; *qu*, quadrate; *so*, supraoccipital; *sq*,  
425 squamosal.

426

427 **Figure 3: Phylogenetic hypothesis of Stereogenyina.**

428 A time-calibrated cladogram depicting a portion of the strict consensus topology of 270 MPTs  
429 with 1134 steps retrieved from the phylogenetic analysis using ordered characters. Dark lines  
430 highlight the known temporal distribution of a taxon and the colored continent symbols highlight  
431 their known spatial distribution. The full tree is provided in the Supplementary File S2.

432

433 **Figure 4: Geographic distribution of stereogenyines.**

434 Section of world map indicating localities of extinct taxa assigned to Stereogenyini. Red circles  
435 indicate Stereogenyita, green circles Bairdemydita, and blue circles non-Stereogenyita and non-  
436 Bairdemydita stereogenyines. 1, *Bairdemys venezuelensis*; 2, *B. thalassica* Ferreira et al., 2015;  
437 3, *B. sanchezi*; 4, *B. winklerae* Gaffney et al., 2008; 5, *B. hartsteini* Gaffney & Wood, 2002; 6,  
438 "*B.*" *healeyorum* Weems & Knight, 2013; 7, *Mogharemys blanckenhorni* (Dacqué, 1912); 8,  
439 *Cordichelys antiqua*; 9, *Latentemys plowdeni*; 10, *Stereogenys cromeri*; 11, *Lemurchelys*  
440 *diasphax* Gaffney et al., 2011; 12, *Brontochelys gaffneyi*; 13, *Shweboemys pilgrimi*; 14, *Piramys*  
441 *auffenbergi*. Abbreviations: EG, Egypt, MM, Myanmar, PK, Pakistan, PR, Puerto Rico, US,  
442 United States of America, VE, Venezuela.

443

# Figure 1

The type locality of *Piramys auffenbergi*.

(A) A simplified map of India. Gujarat State is highlighted in purple, all other states in various shades of grey. (B) Detailed view of the Gulf of Khambhat. Piram Island is highlighted in purple.

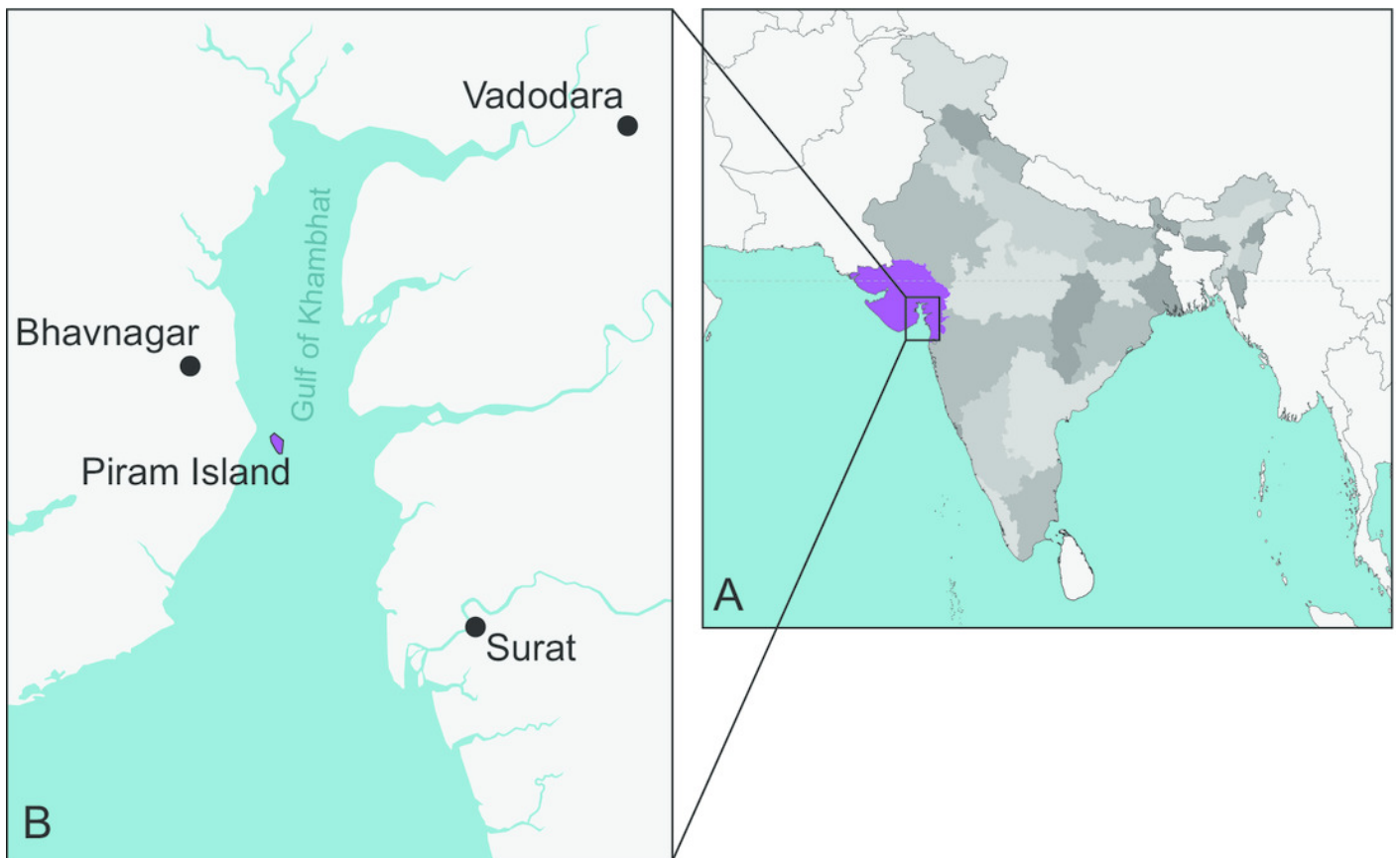


## Figure 2

GSI 18133, *Piramys auffenbergi*, holotype, late Miocene of Piram Island, Gujarat, India.

Photographs and illustrations of specimen in (A) dorsal, (B) right lateral, (C) left lateral, (D) anterior, and (E) posterior views. Abbreviations: *cm*, condylus mandibularis; *et*, Eustachian tube; *fnt*, foramen nervi trigemini; *fr*, frontal; *fst*, foramen stapedio-temporale; *ju*, jugal; *mx*, maxilla; *oc*, occipital condyle; *op*, opisthotic; *pa*, parietal; *pf*, prefrontal; *po*, postorbital; *pr*, prootic; *ptp*, processus trochlearis pterygoidei; *qj*, quadratojugal; *qu*, quadrate; *so*, supraoccipital; *sq*, squamosal.

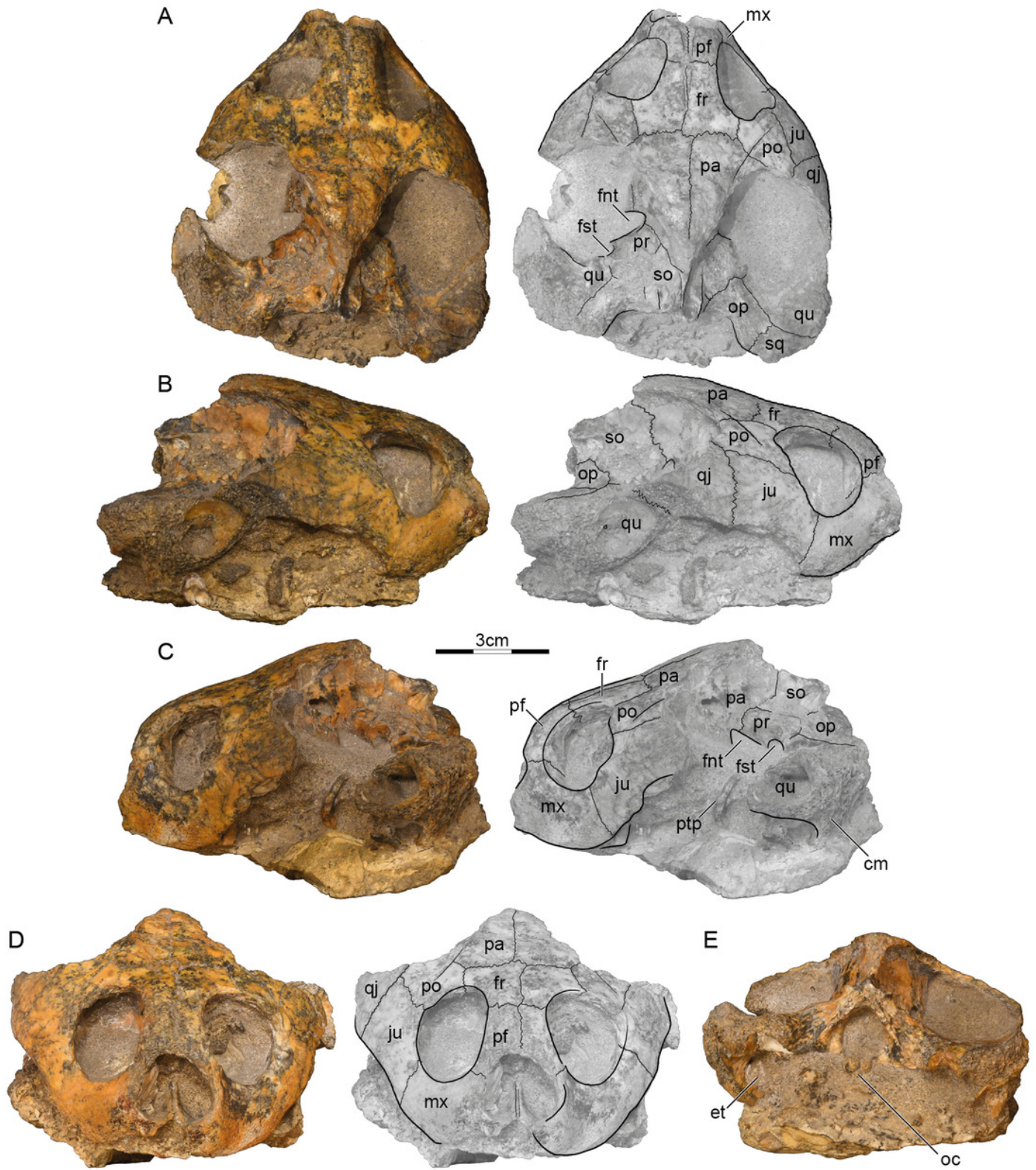


## Figure 3

Phylogenetic hypothesis of Stereogenyina.

A time-calibrated cladogram depicting a portion of the strict consensus topology of 270 MPTs with 1134 steps retrieved from the phylogenetic analysis using ordered characters. Dark lines highlight the known temporal distribution of a taxon and the colored continent symbols highlight their known spatial distribution. The full tree is provided in the Supplementary File S2.

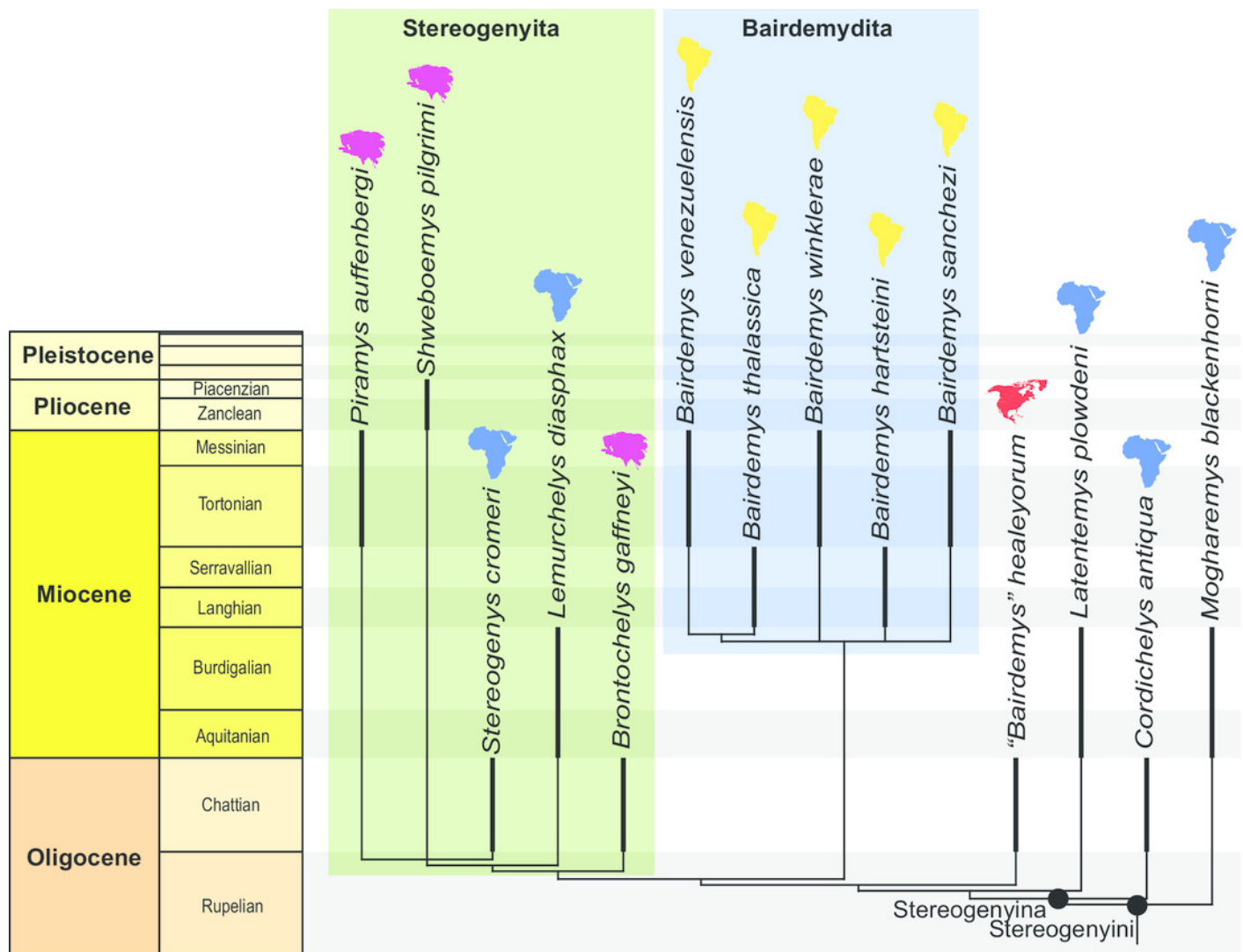


## Figure 4

Geographic distribution of stereogenyines.

Section of world map indicating localities of extinct taxa assigned to Stereogenyini. Red circles indicate Stereogenyita, green circles Bairdemydita, and blue circles non-Stereogenyita and non-Bairdemydita stereogenyines. 1, *Bairdemyys venezuelensis*; 2, *B. thalassica* Ferreira et al., 2015; 3, *B. sanchezi*; 4, *B. winklerae* Gaffney et al., 2008; 5, *B. hartsteini* Gaffney & Wood, 2002; 6, "*B.*" *healeyorum* Weems & Knight, 2013; 7, *Mogharemys blanckenhorni* (Dacqu , 1912); 8, *Cordichelys antiqua*; 9, *Latentemys plowdeni*; 10, *Stereogenys cromeri*; 11, *Lemurchelys diasphax* Gaffney et al., 2011; 12, *Brontochelys gaffneyi*; 13, *Shweboemys pilgrimi*; 14, *Piramys auffenbergi*. Abbreviations: EG, Egypt, MM, Myanmar, PK, Pakistan, PR, Puerto Rico, US, United States of America, VE, Venezuela.

